High order scheme for Schrödinger equation with discontinuous potential I: immersed interfaced method

Hao Wu*

October 21, 2010

Abstract

The immersed interface method is modified to compute the Schrödinger equation with discontinuous potential. By building the jump condition of the solution into the finite difference approximation near the interface, this method could give at least second order convergence rate for the numerical solution on the uniform cartesian grid. The accuracy of this algorithm is tested via several numerical examples.

Key words. Schrödinger equation, discontinuous potential, immersed interface method, finite difference method

1 Introduction

Consider the Schrödinger equation in different forms

$$\text{Stationary} \quad : \quad -\frac{1}{2}\varepsilon^2 \triangle \varphi + V\varphi = E\varphi, \tag{1.1}$$

$$\text{Eigenvalue} \quad : \quad -\frac{1}{2}\varepsilon^2 \triangle \phi + V\phi = E\phi, \tag{1.2}$$

$$\text{Dynamic} \quad : \quad i\varepsilon\psi_t + \frac{1}{2}\varepsilon^2 \triangle \psi = V\psi, \tag{1.3}$$

where ε is re-scaled Plank constant, $\boldsymbol{x} \in \Omega \subset \mathbb{R}^d$ denotes the computational domain, and $V = V(\boldsymbol{x})$ is the potential. We can use different types of boundary conditions, e.g. transparent boundary conditions, periodic boundary conditions and reflection boundary conditions. In stationary problems,

*Department of Mathematical Sciences, Tsinghua University, Beijing, 10084, China(hwu@tsinghua.edu.cn)

the energy E is specified. In eigenvalue problems, the energy E is eigenvalue. In the dynamic problems, we need to specify the initial condition

$$\psi(0, \boldsymbol{x}) = A_0(\boldsymbol{x}) e^{iS_0(\boldsymbol{x})/\varepsilon}. \tag{1.4}$$

Our goal is to compute the wave function $\varphi(\boldsymbol{x})$, $\phi(\boldsymbol{x})$ and $\psi(t, \boldsymbol{x})$ on a uniform Cartesian grid to second order accuracy, even if the discontinuities curves of potential $V(\boldsymbol{x})$ are not aligned with grid.

The Schrödinger equation with discontinuous potential can be used to model the motion of electrons in quantum zones, e.g. quantum barrier, quantum well, quantum dot and p-n junctions [11, 28, 33]. The quantum zones is an active region of the electronic structure, which connects to two highly conduct large reservoirs. And the whole structure is a basic and fundamental semiconductor device in modern industry, e.g. memory chip, microprocessor and integrated circuit [9, 10, 29].

There have been numerous studies on the direct numerical method of the Schrödinger equation, including finite difference method [26, 27, 34], discontinuous Galerkin method [24, 25, 36], spectral type method [7, 8, 13], the WKB scheme [3, 4, 32] and other related technic [1, 2, 5, 16, 31]. However, none of these methods could satisfies all the following requirements for solving the Schrödinger equation with discontinuous potential: (i) at least second order convergence, (ii) robust processing in interface condition, (iii) easy generalization to high dimension (iv) take the advantages of Cartesian grid.

The immersed interface method, original developed for the elliptic equations with discontinuous coefficients and singular sources [12, 17, 19, 20, 21, 22], can maintain at least second order accuracy on the uniform grid even when the discontinuities curves of potential are not aligned with the grid. The idea is to modify the standard finite difference approximation at grid points near interface to keep the jump condition of the derivatives of solutions. Such method has succeed in many applications, e.g. heat equations [6, 23], acoustic wave equations [30, 37], stokes flow and the Navier-Stokes equations [14, 15, 18].

In this paper, we develop the immersed interface method to solve the Schrödinger equation with discontinuous potential. The solution to this method is shown to have at least second order convergence in both one and two dimension. A more interesting question is how to extend such idea for dynamic Schrödinger equation with discontinuous potential in the semiclassical regime. Base on the results here, we will propose two new methods that can achieve high accuracy with low computational cost in a consecutive paper [35].

The paper is organized as follows. In Section 2, we show how the immersed interface method can be used to Schrödinger equation with discontinuous potential. The method in higher space dimensions is given in Section

3. In Section 4, we present the numerical examples to test the accuracy of the method. We make some conclusive remarks in Section 5.

2 One dimensional Schrödinger equation

We begin by considering the one dimensional stationary Schrödinger equation

$$-\frac{1}{2}\varepsilon^2\varphi_{xx} + V\varphi = E\varphi, \tag{2.1}$$

on the computational domain $[a, b]$. The potential $V(x)$ is split into smooth part $V_s(x) \in C^\infty([a, b])$ and discontinuous part $V_d(x)$

$$V(x) = V_s(x) + V_d(x). \tag{2.2}$$

Here the discontinuous potential is given by

$$V_d(x) = \begin{cases} \Delta V, & c_1 < x < c_2, \\ 0, & \text{else.} \end{cases} \tag{2.3}$$

Remark 2.1 *The discontinuous potential $V_d(x)$ can be given in a general form, including more discontinuities for the function and its derivatives. To concentrate on the key idea, we use* (2.3) *in this Section without special instruction.*

Therefore, we have the following jump conditions($s = 1, 2$):

$$\begin{cases} [V]_{c_1} = \Delta V, \quad [V]_{c_2} = -\Delta V, \\ [\varphi]_{c_s} = 0, \quad [\varphi_x]_{c_s} = 0, \\ -\frac{1}{2}\varepsilon^2 [\varphi_{xx}]_{c_s} + [V]_{c_s} \varphi^{c_s} = 0, \end{cases} \tag{2.4}$$

here $[\cdot]_c$ represents the jump in a quantity at the point c

$$[\varphi]_c = \varphi^{c^+} - \varphi^{c^-} = \lim_{x \to c^+} \varphi(x) - \lim_{x \to c^-} \varphi(x).$$

We would like to compute the numerical solution of $\varphi(x)$ on the uniform grid

$$x_n = nh + a, \quad n = 0, 1, \cdots, N,$$

where $h = (b - a)/N$. The point c_s will typically fall between grid points, say

$$x_{m_s} \le c_s \le x_{m_s+1}.$$

We introduce $p_{s1}, p_{s2} \in [0, 1]$ satisfy

$$p_{s1} + p_{s2} = 1, \quad c_s - x_{m_s} = p_{s1}h, \quad x_{m_s+1} - c_s = p_{s2}h.$$

For $n \neq m_s, m_s+1$ the solution is smooth in the interval $[x_{n-1}, x_{n+1}]$, we can use the standard approximation

$$-\frac{1}{2\tau^2}\left(\varphi^{n-1}-2\varphi^n+\varphi^{n+1}\right)+V^n\varphi^n=E\varphi^n,$$

here $\tau=\frac{h}{\varepsilon}$. This gives a local truncation error

$$T^n=-\frac{1}{2}\frac{\varepsilon^2}{h^2}\left(\varphi^{n-1}-2\varphi^n+\varphi^{n+1}\right)+V^n\varphi^n-E\varphi^n=O(h^2).$$

To design the finite difference scheme at $n=m_s$, we firstly have

$$\begin{aligned}
\varphi(x_{m_s-1}) &= \varphi^{c_s}-(p_{s1}+1)h\varphi_x^{c_s}+\frac{1}{2}(p_{s1}+1)^2h^2\varphi_{xx}^{c_s^-}+O(h^3),\\
\varphi(x_{m_s}) &= \varphi^{c_s}-p_{s1}h\varphi_x^{c_s}+\frac{1}{2}p_{s1}^2h^2\varphi_{xx}^{c_s^-}+O(h^3),\\
\varphi(x_{m_s+1}) &= \varphi^{c_s}+p_{s2}h\varphi_x^{c_s}+\frac{1}{2}p_{s2}^2h^2\varphi_{xx}^{c_s^+}+O(h^3)\\
&= \varphi^{c_s}+p_{s2}h\varphi_x^{c_s}+\frac{1}{2}p_{s2}^2h^2\left(\varphi_{xx}^{c_s^-}+\frac{2\left[V\right]_{c_s}}{\varepsilon^2}\varphi^{c_s}\right)+O(h^3),
\end{aligned}$$

and

$$\begin{aligned}
V(x_{m_s})\varphi(x_{m_s}) &= V^{c_s^-}\varphi^{c_s}+O(h),\\
E\varphi(x_{m_s}) &= E\varphi^{c_s}+O(h),\\
-\frac{1}{2}\varepsilon^2\varphi_{xx}^{c_s^-}+V^{c_s^-}\varphi^{c_s} &= E\varphi^{c_s},
\end{aligned}$$

then we can write the modified approximation as [17]

$$\gamma_1^{m_s}\varphi^{m_s-1}+\gamma_2^{m_s}\varphi^{m_s}+\gamma_3^{m_s}\varphi^{m_s+1}+V^{m_s}\varphi^{m_s}=E\varphi^{m_s}. \tag{2.5}$$

This gives the local truncation

$$\begin{aligned}
T^{m_s} &= \gamma_1^{m_s}\varphi(x_{m_s-1})+\gamma_2^{m_s}\varphi(x_{m_s})+\gamma_3^{m_s}\varphi(x_{m_s+1})+V(x_{m_s})\varphi(x_{m_s})-E\varphi(x_{m_s})\\
&= \gamma_1^{m_s}\varphi(x_{m_s-1})+\gamma_2^{m_s}\varphi(x_{m_s})+\gamma_3^{m_s}\varphi(x_{m_s+1})+V^{c_s^-}\varphi^{c_s}-E\varphi^{c_s}+O(h)\\
&= \gamma_1^{m_s}\left(\varphi^{c_s}-(p_{s1}+1)h\varphi_x^{c_s}+\frac{1}{2}(p_{s1}+1)^2h^2\varphi_{xx}^{c_s^-}\right)+\gamma_2^{m_s}\left(\varphi^{c_s}-p_{s1}h\varphi_x^{c_s}+\frac{1}{2}p_{s1}^2h^2\varphi_{xx}^{c_s^-}\right)\\
&\quad+\gamma_3^{m_s}\left(\varphi^{c_s}+p_{s2}h\varphi_x^{c_s}+\frac{1}{2}p_{s2}^2h^2\left(\varphi_{xx}^{c_s^-}+\frac{2\left[V\right]_{c_s}}{\varepsilon^2}\varphi^{c_s}\right)\right)+\frac{1}{2}\varepsilon^2\varphi_{xx}^{c_s^-}+O(h)\\
&= \left(\gamma_1^{m_s}+\gamma_2^{m_s}+\gamma_3^{m_s}\left(1+p_{s2}^2\tau^2\left[V\right]_{c_s}\right)\right)\varphi^{c_s}+\left(-(p_{s1}+1)\gamma_1^{m_s}-p_{s1}\gamma_2^{m_s}+p_{s2}\gamma_3^{m_s}\right)h\varphi_x^{c_s}\\
&\quad+\frac{1}{2}\left((p_{s1}+1)^2\gamma_1^{m_s}+p_{s1}^2\gamma_2^{m_s}+p_{s2}^2\gamma_3^{m_s}+\frac{1}{\tau^2}\right)h^2\varphi_{xx}^{c_s^-}+O(h).
\end{aligned}$$

Then we have the linear system for the coefficients

$$\begin{cases}
\gamma_1^{m_s}+\gamma_2^{m_s}+\gamma_3^{m_s}\left(1+p_{s2}^2\tau^2\left[V\right]_{c_s}\right)=0,\\
-(p_{s1}+1)\gamma_1^{m_s}-p_{s1}\gamma_2^{m_s}+p_{s2}\gamma_3^{m_s}=0,\\
(p_{s1}+1)^2\gamma_1^{m_s}+p_{s1}^2\gamma_2^{m_s}+p_{s2}^2\gamma_3^{m_s}=-\frac{1}{\tau^2}.
\end{cases} \tag{2.6}$$

Similarly as the previous process, we can modify the finite difference approximation at $n = m_s + 1$ as

$$\gamma_1^{m_s+1}\varphi^{m_s} + \gamma_2^{m_s+1}\varphi^{m_s+1} + \gamma_3^{m_s+1}\varphi^{m_s+2} + V^{m_s+1}\varphi^{m_s+1} = E\varphi^{m_s+1}, \quad (2.7)$$

in which the coefficients satisfies

$$\begin{cases} \gamma_1^{m_s+1}\left(1 - p_{s1}^2\tau^2\left[V\right]_{c_s}\right) + \gamma_2^{m_s+1} + \gamma_3^{m_s+1} = 0, \\ -p_{s1}\gamma_1^{m_s+1} + p_{s2}\gamma_2^{m_s+1} + (p_{s2}+1)\,\gamma_3^{m_s+1} = 0, \\ p_{s1}^2\gamma_1^{m_s+1} + p_{s2}^2\gamma_2^{m_s+1} + (p_{s2}+1)^2\gamma_3^{m_s+1} = -\frac{1}{\tau^2}. \end{cases} \quad (2.8)$$

We can simply compute the local truncation error

$$\begin{aligned} T^{m_s+1} &= \gamma_1^{m_s+1}\varphi(x_{m_s}) + \gamma_2^{m_s+1}\varphi(x_{m_s+1}) + \gamma_3^{m_s+1}\varphi(x_{m_s+2}) \\ &\quad + V(x_{m_s+1})\varphi(x_{m_s+1}) - E\varphi(x_{m_s+1}), \\ &= O(h). \end{aligned}$$

Remark 2.2 *As discussed in [17], only four gird points(independent of h) are involved, their $O(h)$ local truncation error is sufficient to ensure the numerical solution converge at least second order.*

For one dimensional eigenvalue problem of Schrödinger equation

$$-\frac{1}{2}\varepsilon^2\phi_{xx} + V\phi = E\phi, \quad (2.9)$$

the potential is given by (2.2)-(2.3), we have same jump condition as (2.4). The numerical solution satisfies

$$-\frac{1}{2\tau^2}\left(\phi^{n-1} - 2\phi^n + \phi^{n+1}\right) + V^n\phi^n = E\phi^n,$$

for $n \neq m_s, m_s + 1$, and

$$\begin{aligned} \gamma_1^{m_s}\phi^{m_s-1} + \gamma_2^{m_s}\phi^{m_s} + \gamma_3^{m_s}\phi^{m_s+1} + V^{m_s}\phi^{m_s} &= E\phi^{m_s}, \\ \gamma_1^{m_s+1}\phi^{m_s} + \gamma_2^{m_s+1}\phi^{m_s+1} + \gamma_3^{m_s+1}\phi^{m_s+2} + V^{m_s+1}\phi^{m_s+1} &= E\phi^{m_s+1}, \end{aligned}$$

where γ_i^m are the solutions of equations (2.6) or (2.8).

At last, we consider the one dimensional dynamic Schrödinger equation

$$i\varepsilon\psi_t + \frac{1}{2}\varepsilon^2\psi_{xx} = V\psi, \quad (2.10)$$

with potential given by (2.2)-(2.3), here $\psi = \psi(t, x)$. The jump condition is similar to (2.4),

$$\begin{cases} \left[V\right]_{c_1} = \Delta V, \quad \left[V\right]_{c_2} = -\Delta V, \\ \left[\psi\right]_{c_s} = 0, \quad \left[\psi_x\right]_{c_s} = 0, \quad \left[\psi_t\right]_{c_s} = 0, \\ -\frac{1}{2}\varepsilon^2\left[\psi_{xx}\right]_{c_s} + \left[V\right]_{c_s}\psi^{c_s} = 0, \end{cases}$$

The time grid is

$$t_l = lk, \quad l = 0, 1, \cdots, L,$$

where $k = T/L$. For $n \neq m_s, m_s + 1$ the solution is smooth in the interval $[x_{n-1}, x_{n+1}]$, the standard Crank-Nicolson approximation can be used

$$\begin{aligned}\frac{\psi^{l+1,n} - \psi^{l,n}}{\omega} &= -\frac{1}{2\tau^2} \cdot \frac{1}{2}\big((\psi^{l+1,n-1} - 2\psi^{l+1,n} + \psi^{l+1,n+1}) \\ &\quad +(\psi^{l,n-1} - 2\psi^{l,n} + \psi^{l,n+1})\big) + \frac{V^n}{2}\left(\psi^{l+1,n} + \psi^{l,n}\right),\end{aligned}$$

with $\omega = \frac{k}{i\varepsilon}$. This gives a local truncation error

$$\begin{aligned}T^{l,n} &= \frac{i\varepsilon}{k}\left(\psi(t_{l+1}, x_n) - \psi(t_l, x_n)\right) + \frac{\varepsilon^2}{4h^2}\left(\psi(t_{l+1}, x_{n-1}) - 2\psi(t_{l+1}, x_n) + \psi(t_{l+1}, x_{n+1})\right) \\ &\quad +\frac{\varepsilon^2}{4h^2}\left(\psi(t_l, x_{n-1}) - 2\psi(t_l, x_n) + \psi(t_l, x_{n+1})\right) - \frac{1}{2}V(x_n)\left(\psi(t_{l+1}, x_n) + \psi(t_l, x_n)\right) \\ &= O(h^2 + k^2).\end{aligned}$$

For $n = m_s$ or $n = m_s + 1$, the modified approximation is

$$\begin{aligned}\frac{\psi^{l+1,m_s} - \psi^{l,m_s}}{\omega} &= \frac{1}{2}\big((\gamma_1^{m_s}\psi^{l+1,m_s-1} + \gamma_2^{m_s}\psi^{l+1,m_s} + \gamma_3^{m_s}\psi^{l+1,m_s+1}) \\ &\quad +(\gamma_1^{m_s}\psi^{l,m_s-1} + \gamma_2^{m_s}\psi^{l,m_s} + \gamma_3^{m_s}\psi^{l,m_s+1})\big) + \frac{V^{m_s}}{2}\left(\psi^{l+1,m_s} + \psi^{l,m_s}\right), \\ \frac{\psi^{l+1,m_s+1} - \psi^{l,m_s+1}}{\omega} &= \frac{1}{2}\big((\gamma_1^{m_s+1}\psi^{l+1,m_s} + \gamma_2^{m_s+1}\psi^{l+1,m_s+1} + \gamma_3^{m_s+1}\psi^{l+1,m_s+2}) \\ &\quad +(\gamma_1^{m_s+1}\psi^{l,m_s} + \gamma_2^{m_s+1}\psi^{l,m_s+1} + \gamma_3^{m_s+1}\psi^{l,m_s+2})\big) \\ &\quad +\frac{V^{m_s+1}}{2}\left(\psi^{l+1,m_s+1} + \psi^{l,m_s+1}\right),\end{aligned}$$

where γ_i^m are the solutions of equations (2.6) and (2.8). Then the local truncations are

$$T^{l,m_s} = O(h + k^2), \quad T^{l,m_s+1} = O(h + k^2).$$

2.1 A special case for δ-potential

In this subsection, we consider the one dimensional stationary Schrödinger equation (1.1)-(2.2) with δ-potential

$$V_d(x) = \Delta V \delta(x - c_1).$$

Then the jump condition is given by

$$[\varphi] = 0, \quad \frac{1}{2}\varepsilon^2\left[\varphi_x\right]_{c_1} = \Delta V \varphi^{c_1}, \quad [\varphi_{xx}] = 0.$$

Using the same idea, we can derive the linear system for the coefficients in approximation (2.5),

$$\begin{cases} \gamma_1^{m_s} + \gamma_2^{m_s} + \gamma_3^{m_s}\,(1 + 2p_{s2}\tau\Delta V/\varepsilon) = 0, \\ -(p_{s1}+1)\gamma_1^{m_s} - p_{s1}\gamma_2^{m_s} + p_{s2}\gamma_3^{m_s} = 0, \\ (p_{s1}+1)^2\gamma_1^{m_s} + p_{s1}^2\gamma_2^{m_s} + p_{s2}^2\gamma_3^{m_s} = -\frac{1}{\tau^2}, \end{cases} \tag{2.11}$$

and in approximation (2.7),

$$\begin{cases} \gamma_1^{m_s+1}\,(1 + 2p_{s1}\tau\Delta V/\varepsilon) + \gamma_2^{m_s+1} + \gamma_3^{m_s+1} = 0, \\ -p_{s1}\gamma_1^{m_s+1} + p_{s2}\gamma_2^{m_s+1} + (p_{s2}+1)\,\gamma_3^{m_s+1} = 0, \\ p_{s1}^2\gamma_1^{m_s+1} + p_{s2}^2\gamma_2^{m_s+1} + (p_{s2}+1)^2\gamma_3^{m_s+1} = -\frac{1}{\tau^2}. \end{cases} \tag{2.12}$$

For eigenvalue problem and dynamic problem, the similar idea has been discussed with coefficients satisfy (2.11) or (2.12).

3 Two dimensional Schrödinger equation

We now consider the two dimensional stationary Schrödinger equation

$$-\frac{1}{2}\varepsilon^2\,(\varphi_{xx} + \varphi_{yy}) + V\varphi = E\varphi, \tag{3.1}$$

on the computational domain $\Omega \subset \mathbb{R}^2$. The potential $V(x)$ is split into smooth part $V_s(x,y) \in C^\infty(\Omega)$ and the discontinuous part $V_d(x,y)$:

$$V(x,y) = V_s(x) + V_d(x), \tag{3.2}$$

$$V_d(x,y) = \begin{cases} \Delta V, & (x,y) \in \Omega_d \subset \Omega, \\ 0, & \text{else.} \end{cases} \tag{3.3}$$

Assume Ω_d is simply connected closed domain and the interface $\Gamma_d = \partial\Omega_d$ is a smooth curve lying in Ω. Therefore, we can define a smooth indicate function $\mathcal{F}(x,y)$ satisfies

$$\begin{aligned} &\mathcal{F}(x,y) > 0, \quad (x,y) \in \Omega_d \setminus \Gamma_d, \\ &\mathcal{F}(x,y) = 0, \qquad (x,y) \in \Gamma_d, \\ &\mathcal{F}(x,y) < 0, \quad (x,y) \in \Omega \setminus \Omega_d. \end{aligned}$$

Remark 3.1 *The discontinuous potential $V_d(x,y)$ and the domain Ω_d can be easily extended into a general form. We make this assumption to simplify the explanation and concentrate on the main idea.*

Let the computational domain be a square, say $[a_1,b_1]\times[a_2,b_2]$. We would like to compute the numerical solution of $\varphi(x,y)$ on the uniform grid

$$\begin{aligned} x_n &= nh + a_1, \qquad n = 0,1,\cdots,N, \\ y_m &= mh + a_2, \qquad m = 0,1,\cdots,M. \end{aligned}$$

where

$$h = \frac{b_1 - a_1}{N} = \frac{b_2 - a_2}{M}.$$

For regular grid points (x_n, y_m) satisfies

$$\mathcal{F}(x_n, y_m)\mathcal{F}(x_{n'}, y_{m'}) > 0, \quad \forall (x_{n'}, y_{m'}) \in S^{n,m},$$
$$S^{n,m} = \{(x_n, y_m),\ (x_{n-1}, y_m),\ (x_{n+1}, y_m),\ (x_n, y_{m-1}),\ (x_n, y_{m+1})\},$$

we can use the standard five points approximation

$$-\frac{\varepsilon^2}{2h^2}\left(\varphi^{n-1,m} + \varphi^{n,m-1} - 4\varphi^{n,m} + \varphi^{n+1,m} + \varphi^{n,m+1}\right) + V^{n,m}\varphi^{n,m} = E\varphi^{n,m},$$

with a local truncation error

$$T^{n,m} = -\frac{\varepsilon^2}{2h^2}\left(\varphi^{n-1,m} + \varphi^{n,m-1} - 4\varphi^{n,m} + \varphi^{n+1,m} + \varphi^{n,m+1}\right) + \left(V^{n,m} - E\right)\varphi^{n,m} = O(h^2).$$

For irregular points, the standard five points are on the different side of the interface, the related approximation is not valid anymore. To design a new finite difference scheme, we firstly look for (x_n^0, y_m^0) on the curve Γ_d who is closest to (x_n, y_m). Taking (x_n^0, y_m^0) as original point, we construct a local coordinate(see Figure 1) with the following transformation

$$\begin{pmatrix} x \\ y \end{pmatrix} = \begin{pmatrix} \cos\theta & -\sin\theta \\ \sin\theta & \cos\theta \end{pmatrix} \begin{pmatrix} \xi \\ \eta \end{pmatrix} + \begin{pmatrix} x_n^0 \\ y_m^0 \end{pmatrix},$$

where ξ and η are in the directions normal and tangential to the interface at

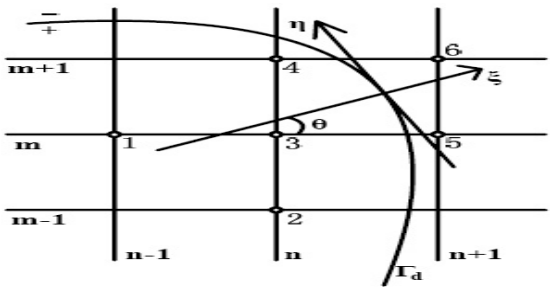

Figure 1: Interface Γ_d in $2d$ domain and the local coordinate (ξ, η).

(x_n^0, y_m^0) respectively, and θ is the rotation angle. The stationary Schrödinger equation (3.1) can be rewritten in the local coordinate as

$$-\frac{1}{2}\varepsilon^2\left(\varphi_{\xi\xi} + \varphi_{\eta\eta}\right) + V\varphi = E\varphi.$$

Then we can give the jump condition at (x_n^0, y_m^0):

$$\begin{cases} [V] = \Delta V, \quad [\varphi] = [\varphi_\xi] = [\varphi_\eta] = 0 \\ [\varphi_{\xi\eta}] = [\varphi_{\eta\eta}] = 0, \quad [\varphi_{\xi\xi}] = \frac{2}{\varepsilon^2}[V]\varphi, \end{cases} \tag{3.4}$$

here $[\cdot]$ represents the jump in a quantity at the point (x_n^0, y_m^0)

$$[\varphi] = \varphi^+ - \varphi^-.$$

We use the superscripts $+$ or $-$ to denote the limiting values of a function from one side (in Ω_d) or the other (in $\Omega \setminus \Omega_d$). It is easy to see there are six constraints, then we need an additional point (x_n^*, y_m^*) to close the system. We choose

$$(x_n^*, y_m^*) \in \widehat{S}^{n,m} = \{(x_{n-1}, y_{m-1}),\ (x_{n-1}, y_{m+1}),\ (x_{n+1}, y_{m-1}),\ (x_{n+1}, y_{m+1})\}$$

be the closest point to (x_n^0, y_m^0). Then we can define

$$S_*^{n,m} = S^{n,m} \cup \{(x_n^*, y_m^*)\},$$
$$S_+^{n,m} = S_*^{n,m} \cap \Omega_d, \quad S_-^{n,m} = S_*^{n,m} \cap (\Omega \setminus \Omega_d).$$

We give Taylor expansion for $(x, y) \in S_{n,m}^+$

$$\varphi(\xi, \eta) = \varphi^+ + \varphi_\xi^+ \xi + \varphi_\eta^+ \eta + \frac{1}{2}\varphi_{\xi\xi}^+ \xi^2 + \varphi_{\xi\eta}^+ \xi\eta + \frac{1}{2}\varphi_{\eta\eta}^+ \eta^2 + O(h^3),$$

and for $(x, y) \in S_{n,m}^-$

$$\varphi(\xi, \eta) = \varphi^- + \varphi_\xi^- \xi + \varphi_\eta^- \eta + \frac{1}{2}\varphi_{\xi\xi}^- \xi^2 + \varphi_{\xi\eta}^- \xi\eta + \frac{1}{2}\varphi_{\eta\eta}^- \eta^2 + O(h^3),$$

here $\varphi, \varphi_\xi^\pm, \varphi_\eta^\pm, \varphi_{\xi\xi}^\pm, \varphi_{\xi\eta}^\pm, \varphi_{\eta\eta}^\pm$ denotes the related limiting values of φ at the point (x_n^0, y_m^0). For $(x_n, y_m) \in S_{n,m}^+$, we have

$$\begin{aligned} V(x_n, y_m)\varphi(x_n, y_m) &= V^+\varphi^+ + O(h), \\ E\varphi(x_n, y_m) &= E\varphi^+ + O(h), \\ -\frac{1}{2}\varepsilon^2\left(\varphi_{\xi\xi}^+ + \varphi_{\eta\eta}^+\right) + V^+\varphi^+ &= E\varphi^+. \end{aligned}$$

We write the modified approximation as

$$\sum_{s \in S_+^{n,m}} \gamma_s^{n,m} \varphi_s^{n,m} + \sum_{s \in S_-^{n,m}} \gamma_s^{n,m} \varphi_s^{n,m} + V^{n,m}\varphi^{n,m} = E\varphi^{n,m}, \tag{3.5}$$

to make the equation clear, we drop the index group (n, m) as

$$\sum_{s \in S_+} \gamma_s \varphi_s + \sum_{s \in S_-} \gamma_s \varphi_s + V\varphi = E\varphi,$$

then the local truncation is given by

$$\begin{aligned}
T &= \sum_{s\in S_+}\gamma_s\varphi(x_s,y_s)+\sum_{s\in S_-}\gamma_s\varphi(x_s,y_s)+(V(x_n,y_m)-E)\varphi(x_n,y_m)\\
&= \sum_{s\in S_+}\gamma_s\left(\varphi^++\varphi^+_\xi\xi_s+\varphi^+_\eta\eta_s+\frac{1}{2}\varphi^+_{\xi\xi}\xi_s^2+\varphi^+_{\xi\eta}\xi_s\eta_s+\frac{1}{2}\varphi^+_{\eta\eta}\eta_s^2\right)+\left(V^+-E\right)\varphi^+\\
&\quad+\sum_{s\in S_-}\gamma_s\left(\varphi^-+\varphi^-_\xi\xi_s+\varphi^-_\eta\eta_s+\frac{1}{2}\varphi^-_{\xi\xi}\xi_s^2+\varphi^-_{\xi\eta}\xi_s\eta_s+\frac{1}{2}\varphi^-_{\eta\eta}\eta_s^2\right)+O(h)\\
&= \sum_{s\in S_+}\gamma_s\left(\varphi^++\varphi^+_\xi\xi_s+\varphi^+_\eta\eta_s+\frac{1}{2}\varphi^+_{\xi\xi}\xi_s^2+\varphi^+_{\xi\eta}\xi_s\eta_s+\frac{1}{2}\varphi^+_{\eta\eta}\eta_s^2\right)+\frac{1}{2}\varepsilon^2\left(\varphi^+_{\xi\xi}+\varphi^+_{\eta\eta}\right)\\
&\quad+\sum_{s\in S_-}\gamma_s\left(\varphi^++\varphi^+_\xi\xi_s+\varphi^+_\eta\eta_s+\frac{1}{2}\left(\varphi^+_{\xi\xi}-\frac{2}{\varepsilon^2}\left[V\right]\varphi^+\right)\xi_s^2+\varphi^+_{\xi\eta}\xi_s\eta_s+\frac{1}{2}\varphi^+_{\eta\eta}\eta_s^2\right)+O(h).
\end{aligned}$$

This gives the linear system for the coefficients

$$\begin{cases}
\sum_{s\in S_*}\gamma_s-\frac{[V]}{\varepsilon^2}\sum_{s\in S_-}\xi_s^2\gamma_s=0, & \sum_{s\in S_*}\xi_s^2\gamma_s=-\varepsilon^2,\\
\sum_{s\in S_*}\xi_s\gamma_s=0, & \sum_{s\in S_*}\xi_s\eta_s\gamma_s=0,\\
\sum_{s\in S_*}\gamma_s\eta_s=0, & \sum_{s\in S_*}\eta_s^2\gamma_s=-\varepsilon^2.
\end{cases}\tag{3.6}$$

For $(x_n,y_m)\in S_-^{n,m}$, we have

$$\begin{aligned}
V(x_n,y_m)\varphi(x_n,y_m) &= V^-\varphi^-+O(h),\\
E\varphi(x_n,y_m) &= E\varphi^-+O(h),\\
-\frac{1}{2}\varepsilon^2\left(\varphi^-_{\xi\xi}+\varphi^-_{\eta\eta}\right)+V^-\varphi^- &= E\varphi^-.
\end{aligned}$$

then the coefficients for the modified approximation (3.5) is given by

$$\begin{cases}
\sum_{s\in S_*}\gamma_s+\frac{[V]}{\varepsilon^2}\sum_{s\in S_+}\xi_s^2\gamma_s=0, & \sum_{s\in S_*}\xi_s^2\gamma_s=-\varepsilon^2,\\
\sum_{s\in S_*}\xi_s\gamma_s=0, & \sum_{s\in S_*}\xi_s\eta_s\gamma_s=0,\\
\sum_{s\in S_*}\eta_s\gamma_s=0, & \sum_{s\in S_*}\eta_s^2\gamma_s=-\varepsilon^2,
\end{cases}\tag{3.7}$$

and the related local truncation error is

$$\begin{aligned}
T &= \sum_{s\in S_+}\gamma_s\varphi(x_s,y_s)+\sum_{s\in S_-}\gamma_s\varphi(x_s,y_s)+(V(x_n,y_m)-E)\varphi(x_n,y_m)\\
&= O(h).
\end{aligned}$$

Remark 3.2 *As discussed in [17], the irregular points, which are adjacent to the curve Γ_d, form a lower-dimensional set. Their $O(h)$ local truncation error is sufficient to ensure the numerical solution converge at least second order, just as in one dimension.*

For two dimensional eigenvalue problem of Schrödinger equation

$$-\frac{1}{2}\varepsilon^2\left(\phi_{xx}+\phi_{yy}\right)+V\phi=E\phi, \tag{3.8}$$

the potential is given by (3.2)-(3.3), we have same jump condition as (3.4). The numerical solution satisfies

$$-\frac{\varepsilon^2}{2h^2}\left(\phi^{n-1,m}+\phi^{n,m-1}-4\phi^{n,m}+\phi^{n+1,m}+\phi^{n,m+1}\right)+V^{n,m}\phi^{n,m}=E\phi^{n,m},$$

for regular points, and

$$\sum_{s\in S_+^{n,m}}\gamma_s^{n,m}\phi_s^{n,m}+\sum_{s\in S_-^{n,m}}\gamma_s^{n,m}\phi_s^{n,m}+V^{n,m}\phi^{n,m}=E\phi^{n,m},$$

for irregular points, where $\gamma_s^{n,m}$ are the solutions of equation (3.6) or (3.7).

At last, we consider the two dimensional dynamic Schrödinger equation

$$i\varepsilon\psi_t+\frac{1}{2}\varepsilon^2\left(\psi_{xx}+\psi_{yy}\right)=V\psi, \tag{3.9}$$

with potential given by (3.2)-(3.3), here $\psi=\psi(t,x,y)$. The jump condition is similar to (3.4),

$$\begin{cases}\ [V]=\Delta V, \quad [\varphi]=[\varphi_t]=[\varphi_\xi]=[\varphi_\eta]=0\\ \ [\varphi_{\xi\eta}]=[\varphi_{\eta\eta}]=0, \quad [\varphi_{\xi\xi}]=\frac{2}{\varepsilon^2}[V]\,\varphi,\end{cases}$$

The time grid is

$$t_l=lk, \quad l=0,1,\cdots,L,$$

where $k=T/L$. For regular points, the standard Crank-Nicolson approximation can be used

$$\begin{aligned}&\frac{i\varepsilon}{\Delta t}\left(\psi^{l+1,n,m}-\psi^{l,n,m}\right)\\ =\ &-\frac{\varepsilon^2}{4h^2}\left(\psi^{l+1,n-1,m}+\psi^{l+1,n,m-1}-4\psi^{l+1,n,m}+\psi^{l+1,n+1,m}+\psi^{l+1,n,m+1}\right)\\ &-\frac{\varepsilon^2}{4h^2}\left(\psi^{l,n-1,m}+\psi^{l,n,m-1}-4\psi^{l,n,m}+\psi^{l,n+1,m}+\psi^{l,n,m+1}\right)+\frac{V^{n,m}}{2}\left(\psi^{l+1,n,m}+\psi^{l,n,m}\right),\end{aligned}$$

this gives a local truncation error

$$T^{l,n,m}=O(h^2+k^2).$$

For irregular points, the modified approximation is

$$\begin{aligned}&\frac{i\varepsilon}{\Delta t}\left(\psi^{l+1,n,m}-\psi^{l,n,m}\right)-\frac{V^{n,m}}{2}\left(\psi^{l+1,n,m}+\psi^{l,n,m}\right)\\ =\ &-\frac{1}{2}\Big(\sum_{s\in S_+^{n,m}}\gamma_s^{n,m}\left(\psi_s^{l+1,n,m}+\psi_s^{l,n,m}\right)+\sum_{s\in S_-^{n,m}}\gamma_s^{n,m}\left(\psi_s^{l+1,n,m}+\psi_s^{l,n,m}\right)\Big),\end{aligned}$$

where $\gamma_s^{n,m}$ are the solutions of equation (3.6) or (3.7). Then the local truncation error is

$$T^{l,n,m}=O(h+k^2).$$

h	$\frac{1}{200}$	$\frac{1}{400}$	$\frac{1}{800}$	$\frac{1}{1600}$
$E = 0.5$	1.44×10^{-3}	3.86×10^{-4}	7.57×10^{-5}	1.76×10^{-5}
$E = 1.0$	4.73×10^{-3}	1.18×10^{-3}	2.88×10^{-4}	5.73×10^{-5}
$E = 1.5$	8.72×10^{-3}	2.17×10^{-3}	5.12×10^{-4}	1.03×10^{-4}

Table 1: Example 1-1, the l^∞ errors of $\varphi(x)$ for different energy E and mesh size h.

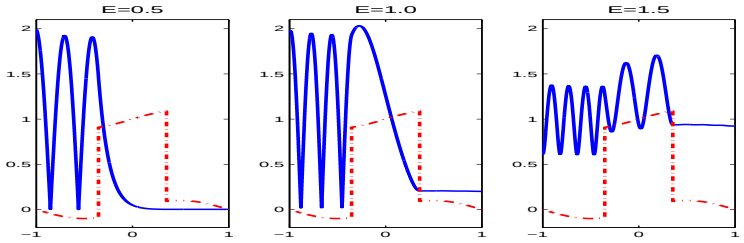

Figure 2: Example 1-1, The wave amplitude $|\varphi(x)|$(blue solid line) for different energy E, the red dash-dot line are the potential.

4 Numerical examples

In this section, we will present a few examples to test the order of accuracy for the numerical scheme. In all the examples, the 'exact' Schrödinger solution is obtained by using standard finite difference approximation with a very fine mesh size and a very small time step.

Example 1. We consider one dimensional Schrödinger equation with the following parameters

$$a = -1,\ b = 1,\ c_1 = -\tfrac{\sqrt{2}}{4},\ c_2 = \tfrac{\sqrt{2}}{4},$$
$$\Delta V = 1,\ V_s(x) = 0.1 \sin \pi x.$$

(1) For stationary Schrödinger equation (2.1) with transparent boundary condition

$$\begin{aligned} \varepsilon\varphi_x(a) + i\sqrt{2(E - V(a))}\varphi(a) &= 2i\sqrt{2(E - V(a))}, \\ \varepsilon\varphi_x(b) - i\sqrt{2(E - V(b)))}\varphi(b) &= 0, \end{aligned} \tag{4.1}$$

here $\varepsilon = 0.1$, we output the l^∞ errors of wave function for different energy E and mesh size h in Table 1. In Figure 2, the wave amplitude $|\varphi(x)|$ are plotted versus different energy E.

(2) For eigenvalue problem of Schrödinger equation (2.9) with periodic boundary condition(pbc)

$$\phi(x + (b - a)) = \phi(x),$$

h	$\frac{1}{200}$	$\frac{1}{400}$	$\frac{1}{800}$	$\frac{1}{1600}$
pbc	1.92×10^{-3}	4.82×10^{-4}	1.09×10^{-4}	2.26×10^{-5}
rbc	1.97×10^{-3}	4.95×10^{-4}	1.12×10^{-4}	2.32×10^{-5}

Table 2: Example 1-2, the l^∞ errors of $\phi(x)$ for different mesh size h.

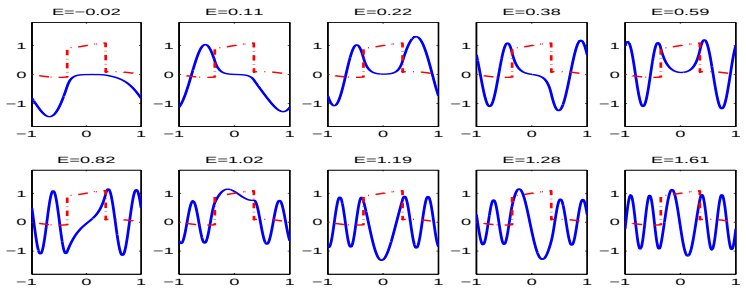

(a) Periodic boundary condition

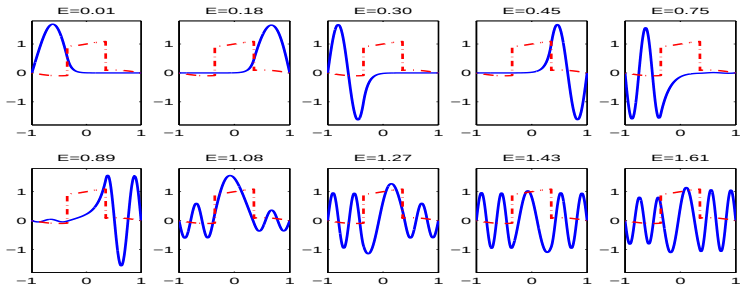

(b) Reflection boundary condition

Figure 3: Example 1-2, The wave function of first ten eigenvectors $\phi(x)$.

or reflection boundary condition(rbc)

$$\phi(a) = \phi(b) = 0,$$

here $\varepsilon = 0.1$, we output the l^∞ errors of the first ten eigenvectors for different mesh size h in Table 2. In Figure 3, the wave function of first ten eigenvectors $\phi(x)$ are plotted.

(3) For dynamic Schrödinger equation (2.10) with periodic boundary condition(pbc)

$$\psi(t, x + (b - a)) = \psi(t, x),$$

or reflection boundary condition(rbc)

$$\psi(t, a) = \psi(t, b) = 0,$$

here $\varepsilon = 0.02$, $T_f = 0.54$, and the initial data is given by

$$\psi_0(x) = e^{-400(x+0.6)^2} e^{i(x+1)/\varepsilon},$$

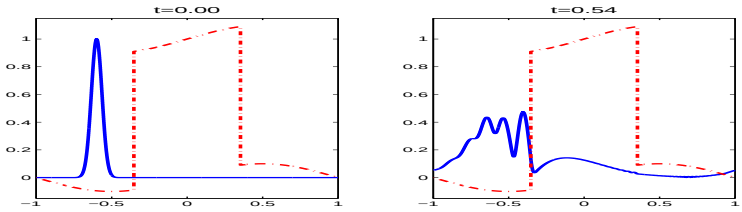

(a) Periodic boundary condition

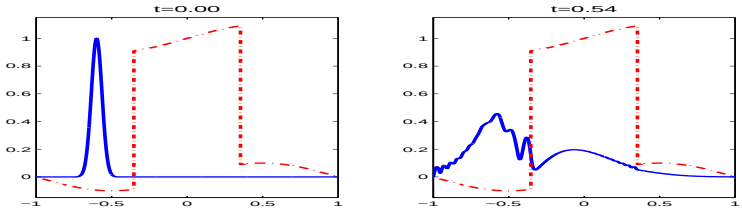

(b) Reflection boundary condition

Figure 4: Example 1-3, The initial and final wave amplitude $|\psi(t,x)|$.

h	$\frac{1}{1000}$	$\frac{1}{2000}$	$\frac{1}{4000}$	$\frac{1}{8000}$
pbc	9.23×10^{-4}	2.34×10^{-4}	5.58×10^{-5}	1.11×10^{-5}
rbc	1.52×10^{-3}	3.90×10^{-4}	9.15×10^{-5}	1.79×10^{-5}

Table 3: Example 1-3, the l^∞ errors of $\psi(t,x)$ for different mesh size h.

we out the the l^∞ errors of the wave function for different mesh size h at time $t=T_f$ in Table 3. In Figure 4, the wave amplitude $|\psi(t,x)|$ are plotted. From all these data, we can observe that the numerical solutions converge at second order.

Example 2. We consider one dimensional Schrödinger equation on the computational domain $[-1,1]$ with δ-potential

$$V(x)=2(x-\frac{\sqrt{3}}{20})^2-1+\frac{1}{10}\delta(x-\frac{\sqrt{3}}{20}).$$

(1) For stationary Schrödinger equation (2.1) with transparent boundary condition (4.1), here $\varepsilon=0.1$, we output the l^∞ errors of wave function for different mesh size h in Table 4. In Figure 5, the real and imaginary part of wave function $\varphi(x)$ are plotted.

(2) For eigenvalue problem of Schrödinger equation (2.9) with reflection boundary condition, here $\varepsilon=0.1$, we output the l^∞ errors of the first six eigenvectors for different mesh size h in Table 5. In Figure 6, the wave function of first six eigenvectors $\phi(x)$ are plotted.

h	$\frac{1}{200}$	$\frac{1}{400}$	$\frac{1}{800}$	$\frac{1}{1600}$
$E = 1.5$	9.33×10^{-3}	2.31×10^{-3}	5.47×10^{-4}	1.11×10^{-4}

Table 4: Example 2-1, the l^∞ errors of $\varphi(x)$ for different mesh size h.

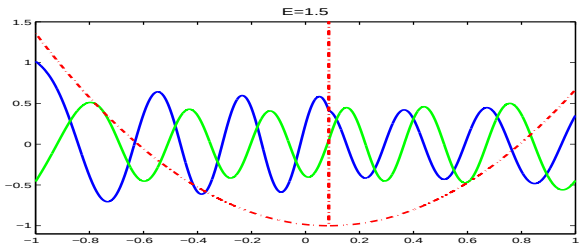

Figure 5: Example 2-1, The real part(blue solid line) and imaginary part(green solid line) of wave function $\varphi(x)$ for energy $E = 1.5$, the red dash-dot line are the potential.

h	$\frac{1}{200}$	$\frac{1}{400}$	$\frac{1}{800}$	$\frac{1}{1600}$
rbc	2.00×10^{-3}	5.00×10^{-4}	1.18×10^{-4}	2.45×10^{-5}

Table 5: Example 2-2, the l^∞ errors of $\phi(x)$ for different mesh size h.

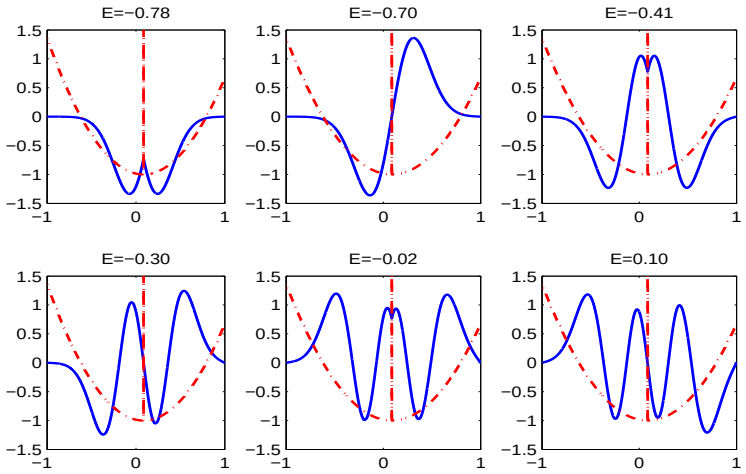

Figure 6: Example 2-2, The wave function of first six eigenvectors $\phi(x)$.

h	$\frac{1}{1000}$	$\frac{1}{2000}$	$\frac{1}{4000}$	$\frac{1}{8000}$
pbc	4.65×10^{-2}	1.11×10^{-2}	2.61×10^{-3}	5.21×10^{-4}

Table 6: Example 2-3, the l^∞ errors of $\psi(t,x)$ for different mesh size h.

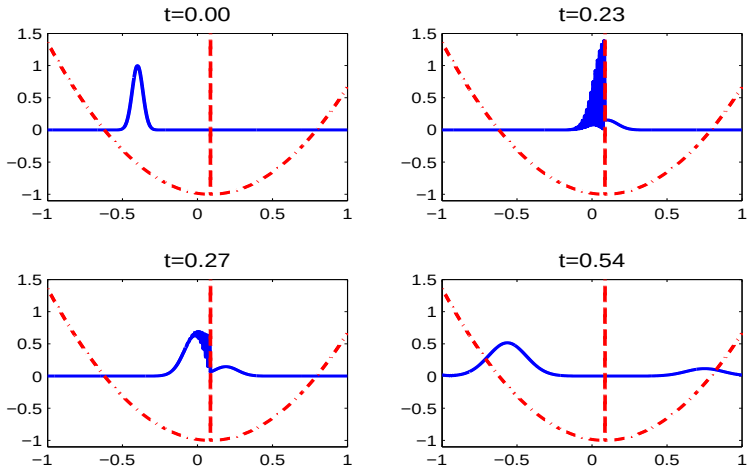

Figure 7: Example 2-3, The wave amplitude $|\psi(t,x)|$ at different time.

(3) For dynamic Schrödinger equation (2.10) with periodic boundary condition, here $\varepsilon = 0.01,\ T_f = 0.54$, and the initial data is given by

$$\psi_0(x) = e^{-400(x+0.4)^2} e^{2i(x+1)/\varepsilon},$$

we out the the l^∞ errors of the wave function for different mesh size h at time $t = T_f$ in Table 6. In Figure 7, the wave amplitude $|\psi(t,x)|$ are plotted at time $t = 0,\ 0.23,\ 0.27,\ 0.54$. From which, we can draw the same conclusion as in Example 1.

Example 3. We consider two dimensional Schrödinger equation on the computational domain $\Omega = [-0.5, 1] \times [-0.5, 0.5]$ with potential

$$V(x,y) = \begin{cases} 0.3, & (x-0.5)^2 + y^2 < 0.093, \\ 0, & \text{else.} \end{cases}$$

(1) For stationary Schrödinger equation (3.1) with boundary condition

$$\begin{aligned} \varphi(x, \pm 0.5) &= 0, \\ \varepsilon \partial_x \varphi(-0.5, y) &= \sum_{E > E_k} i\sqrt{2(E-E_k)}(2a_k - \varphi_k^l)\chi_k(y) + \sum_{E \le E_k} \sqrt{2(E_k - E)}\varphi_k^l \chi_k(y), \\ \varepsilon \partial_x \varphi(1, y) &= \sum_{E > E_k} i\sqrt{2(E-E_k)}\varphi_k^r \chi_k(y) - \sum_{E \le E_k} \sqrt{2(E_k - E)}\varphi_k^r \chi_k(y), \end{aligned}$$

k	1	2	3	4	5	6
E_k	0.049	0.197	0.444	0.790	1.234	1.777

Table 7: Example 3-1, the first six eigenvalues of (4.2).

h	$\frac{1}{40}$	$\frac{1}{80}$	$\frac{1}{160}$
$E = 0.2$	3.88×10^{-2}	9.04×10^{-3}	1.79×10^{-3}
$E = 0.4$	3.42×10^{-2}	8.29×10^{-3}	1.69×10^{-3}
$E = 0.6$	5.23×10^{-2}	1.26×10^{-2}	2.53×10^{-3}

Table 8: Example 3-1, the l^∞ errors of $|\varphi(x, y)|$ for different energy E and mesh size h.

here $(E_k, \chi_k(y))$ are solutions of the eigenvalue problem

$$\begin{cases} -\frac{1}{2}\varepsilon^2 \partial_{yy}\chi(y) = E\chi(y), \\ \chi(\pm 0.5) = 0, \ \langle \chi(y), \chi(y) \rangle = 1, \end{cases} \tag{4.2}$$

and

$$\varphi(-0.5, y) = \sum_{k=1}^{\infty} \varphi_k^l \chi_k(y), \quad \text{with} \quad \varphi_k^l = \langle \varphi(-0.5, y), \chi_k(y) \rangle,$$
$$\varphi(1, y) = \sum_{k=1}^{\infty} \varphi_k^r \chi_k(y), \quad \text{with} \quad \varphi_k^r = \langle \varphi(1, y), \chi_k(y) \rangle.$$

The re-scaled Planck constant is $\varepsilon = 0.1$. In Table 7, we present first six eigenvalues of (4.2). From which, we can believe that the truncation of infinite series for the boundary condition is accurate enough at $K = 6$ when $E \leq 0.7$. The coefficients of incoming wave a_k are given by

$$a_k = \begin{cases} 1, & k = 1, 2, \\ 0, & \text{else.} \end{cases}$$

We output the l^∞ errors of wave amplitude for different energy E and mesh size h in Table 8. In Figure 8, the wave amplitude $|\varphi(x, y)|$ are plotted versus different energy E.

(2) For eigenvalue problem of Schrödinger equation (3.8) with boundary condition,

$$\begin{aligned} \phi(x, \pm 0.5) &= 0, \\ \phi(x + 1.5, y) &= \phi(x, y), \end{aligned}$$

here $\varepsilon = 0.1$, we output the l^∞ errors of the first six eigenvalues and eigenvectors for different mesh size h in Table 9. In Figure 9, the wave amplitude of first six eigenvectors $|\phi(x, y)|$ are plotted.

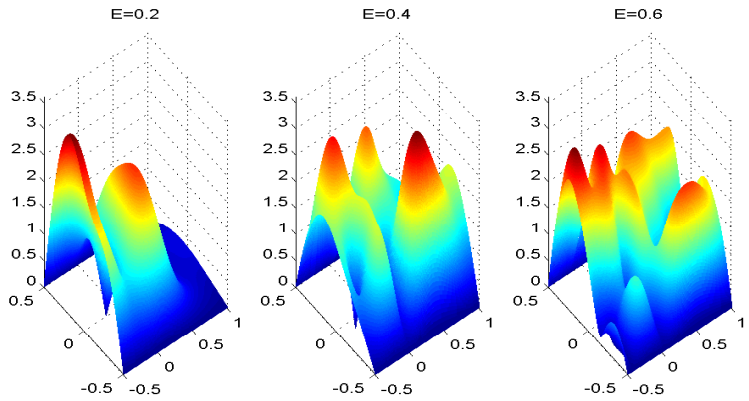

Figure 8: Example 3-1, The wave amplitude $|\varphi(x, y)|$ for different energy E.

h	$\frac{1}{40}$	$\frac{1}{80}$	$\frac{1}{160}$
l^∞ error of E	5.45×10^{-4}	1.28×10^{-4}	2.57×10^{-5}
l^∞ error of $\lvert\phi(x)\rvert$	6.70×10^{-2}	1.65×10^{-2}	4.02×10^{-3}

Table 9: Example 3-2, the l^∞ errors of E and $|\phi(x, y)|$ for different mesh size h.

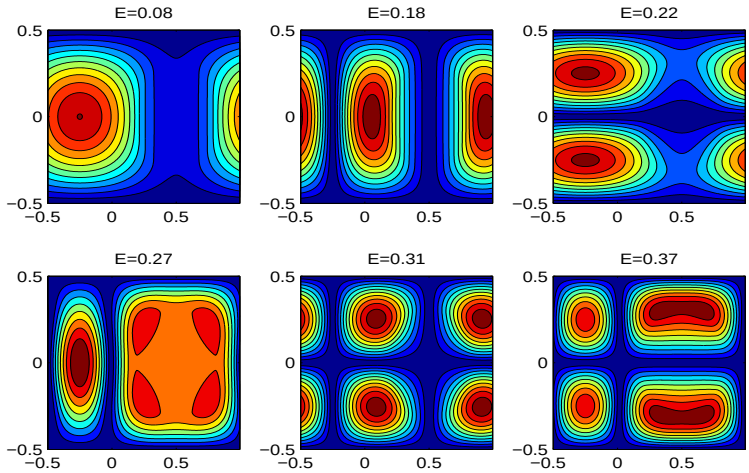

Figure 9: Example 3-2, The wave amplitude of first six eigenvectors $|\phi(x, y)|$.

h	$\frac{1}{40}$	$\frac{1}{80}$	$\frac{1}{160}$
l^∞ error	1.19×10^{-1}	2.90×10^{-2}	6.79×10^{-3}

Table 10: Example 3-3, the l^∞ errors of $|\psi(t,x,y)|$ for different mesh size h.

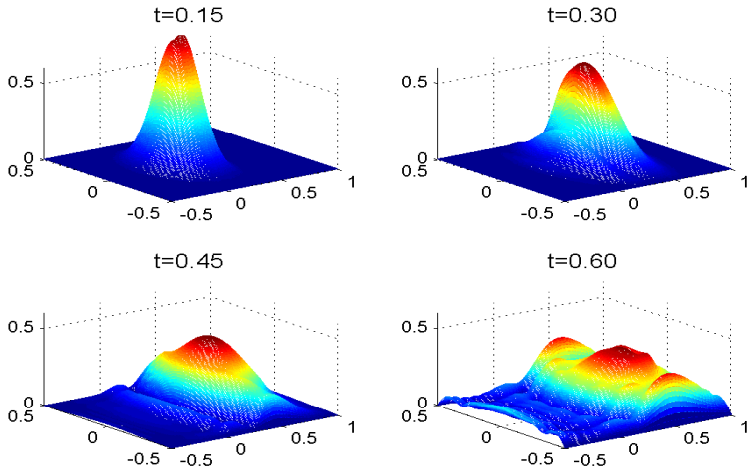

Figure 10: Example 3-3, The wave amplitude of $|\psi(t,x,y)|$.

(3) For dynamic Schrödinger equation (3.9) with boundary condition,

$$\begin{aligned} \psi(t,x,\pm 0.5) &= 0, \\ \psi(t,x+1.5,y) &= \psi(x,y), \end{aligned}$$

here $\varepsilon = 0.05$, $T_f = 0.6$, and the initial data is given by

$$\psi_0(x,y) = e^{-40\left((x+0.05)^2+y^2\right)} e^{1.2i(x+1)/\varepsilon},$$

we out the the l^∞ errors of the wave amplitude for different mesh size h at time $t = T_f$ in Table 10. In Figure 10, the wave amplitude $|\psi(t,x,y)|$ are plotted at time $t = 0.15,\ 0.3,\ 0.45,\ 0.6$. From which, we can draw the same conclusion as in Example 1.

5 Conclusion

Since the discontinuous potential would effect the continuity of wave function's derivatives, the standard numerical methods for Schrödinger equation with discontinuous potential give low accuracy. On the other hand, the Schrödinger equation with discontinuous potential is a basic model in many practical applications, a high order numerical method is required. For this

reason, we modify the famous immersed interface method to give a second order convergence scheme for the Schrödinger equation with discontinuous potential. By serval numerical examples, we verify this method.

The issue of computing dynamic Schrödinger equation with discontinuous potential in the semiclassical regime is itself an interesting topic which will be studied in a forthcoming paper [35]. Another interesting problem is how to modify the immersed interface method so that the mass and energy conservation can be preserved in computing the dynamic Schrödinger equation with discontinuous potential. This topic is still under investigation.

Acknowledgement

During this research, H. Wu benefited from a Post Doc position supported by the Conseil regional Midi Pyrénées (http://www.midipyrenees.fr/) entitled "Méthodes Numériques Multi-échelles pour le transport quantique" and by the ANR Project No. BLAN07-2 212988 entitled "QUATRAIN"). H. Wu would also acknowledge support from NSFC Projects 11071139 and NSFC Projects 10971115.

References

[1] N. Ben Abdallah, *On a multidimensional Schrödinger-Poisson scattering model for semiconductors*, Joural of Mathematical Physics, 41(2000), no. 7, 4241-4261.

[2] N. Ben Abdallah, P. Degond and P.A. Markowich, *On a one-dimensional Schrödinger-Poisson scattering model*, Z. angew. Math. Phys., 48(1997), 135-155.

[3] N. Ben Abdallah, C. Negulescu, M. Mouis and E. Polizzi, *Simulation Schemes in 2D Nanoscale MOSFETs: A WKB Based Method*, Journal of Computational Electronics, 3(2004), 397C400.

[4] N. Ben Abdallah and O. Pinaud, *Multiscale simulation of transport in an open quantum system: Resonances and WKB interpolation*, Journal of Computational Physics, 213(2006), no. 1, 288-310.

[5] N. Ben Abdallah and H. Wu, *A generalized stationary algorithm for resonant tunneling: multi-mode approximation and high dimension*, Communications in Computational Physics, to appear.

[6] L. Adams and Z.L. Li, *The immersed interface/multigrid methods for interface problems*, SIAM Journal on Scientific Computing, 24(2002), no. 2, 463-479.

[7] W.Z. Bao, S. Jin and P.A. Markowich, *On time-splitting spectral approximations for the Schrödinger equation in the semiclassical regime*, Journal of Computational Physics, 175(2002), 487-524.

[8] W.Z. Bao, S. Jin and P.A. Markowich, *Numerical studies of time-splitting spectral discretizations of nonlinear Schrödinger equations in the semiclassical regime*, SIAM Journal on Scientific Computing, 25(2003), no. 1, 27-64.

[9] S. Datta, *Electronic Transport in Mesoscopic Systems*, Cambridge University Press, 1995.

[10] S. Datta, *Quantum Transport: Atom to Transistor*, Cambridge University Press, 2005.

[11] P. Harrison, *Quantum wells, wires and dots: theoretical and computational physics of semiconductor nanostructures*, Jonh Wiley & Sons, New York, 2000.

[12] H.X. Huang and Z.L. Li, *Convergence analysis of the immersed interface method*, IMA Journal of Numerical Analysis, 19(1999), 583-608.

[13] T. Jahnke and C. Lubich, *Error bounds for exponential operator splittings*, BIT, 40(2000), no. 4, 735-744.

[14] M.C. Lai and Z.L. Li, *The immersed interface method for the Navier-Stokes equations with singular forces*, Journal of Computational Physics, 171(2001), 822-842.

[15] L. Lee and R.J. LeVeque, *An immersed interface method for incompressible Navier-Stokes equations*, SIAM Journal on Scientific Computing, 25(2003), no. 3, 832-856.

[16] C. Lent and D. Kirkner, *The quantum transmitting boundary method*, J. Appl. Phys., 67(1990), 6353-6359.

[17] R.J. Leveque and Z.L. Li, *The immersed interface method for elliptic equations with discontinuous coefficients and singular sources*, SIAM Journal on Numerical Analysis, 31(1994), no. 4, 1019-1044.

[18] R.J. Leveque and Z.L. Li, *Immersed interface method for Stokes flow with elastic boundaries or surface tension*, SIAM Journal on Scientific Computing, 18(1997), 709-735.

[19] Z.L. Li, *A note on immersed interface methods for three dimensional elliptic equations*, Computers & Mathematics with Applications, 31(1996), no. 3, 9-17.

[20] Z.L. Li, *A fast iterative algorithm for elliptic interface problems*, SIAM Journal on Numerical Analysis, 35(1998), no. 1, 230-254.

[21] Z.L. Li, *The immersed interface method using a finite element formulation*, Applied Numerical Mathematics, 27(1998), 253-267.

[22] Z.L. Li and K. Ito, *Maximum principle preserving schemes for interface problems with discontinuous coefficients*, SIAM Journal on Scientific Computing, 23(2001), no. 1, 339-361.

[23] Z.L. Li and A. Mayo, *ADI methods for heat equations with discontinuties along an arbitrary interface*, Proceedings of Symposia in Applied Mathematics, 48(1993), 311-315.

[24] T. Lu and W. Cai, *A Fourier spectral-discontinuous Galerkin method for time-dependent 3-D Schrödinger-Poisson equations with discontinuous potentials*, Journal of Computational and Applied Mathematics, 220(2008), 588-614.

[25] T. Lu, W. Cai and P.W. Zhang, *Conservative local discontinuous Galerkin methods for time dependent Schrödinger equation*, International Journal of numerical analysis and Modeling, 2(2005), no. 1, 75-84.

[26] P.A. Markowich, P. Pietra and C. Pohl, *Numerical approximation of quadratic obaservables of Schrödinger-type equations in the semiclassical limit*, Numerische Mathematik, 81(1999), no. 4, 595-630.

[27] P.A. Markowich, P. Pietra, C. Pohl and H.P. Stimming, *A wigner-measure analysis of the Dufort-Frankel scheme for the Schrödinger equation*, SIAM Journal on Numerical Analysis, 40(2002), no. 4, 1281-1310.

[28] P.A. Markowich, C. Ringhofer and C. Schmeiser, *Semiconductor Equations*, Springer Verlag Wien, 1990.

[29] H. Mizuta and T. Tanou, *The Physics and Applications of Resonant Tunnelling Diodes*, Cambridge University Press, 1995.

[30] J. Piraux and B. Lombard, *A new interface method for hyperbolic problems with discontinuous coefficients. One-dimensional acoustic example*, Journal of Computational Physics, 168(2001), 227-248.

[31] E. Polizzi and N. Ben Abdallah, *Subband decomposition approach for the simulation of quantum electron transport in nanostructures*, Journal of Computational Physics 202(2005), no. 1, 150-180.

[32] W. Wang and C.W. Shu, *The WKB local discontinuous Galerkin method for the simulation of Schrödinger equation in a resonant tunneling diode*, Journal of Scientific Computing, 40(2009), no. 1-3, 360-374.

[33] C. Weisbuch and B. Vinter, *Quantum Semiconductor Structures: Fundamentals and Applications*, Academic Press, 1991.

[34] L.X. Wu, *Dufort-Frankel-type methods for linear and nonlinear Schrödinger equations*, SIAM Journal on Numerical Analysis, 33(1996), no. 4, 1526-1533.

[35] H. Wu, *High order scheme for Schrödinger equation with discontinuous potential II: efficient improvement for dynamic problems in the semiclassical regime*, preprint.

[36] Y. Xu and C.W. Shu, *Local discontinuous Galerkin methods for nonlinear Schrödinger equations*, Journal of Computational Physics, 205(2005), 72C97.

[37] C.M. Zhang and R.J. LeVeque, *The immersed interface method for acoustic wave equations with discontinuous coefficients*, Wave Motion, 25(1997), 237-263.